A Concept for Torque Modulation-Based Train-Borne Measurement of Coefficient of Friction

Krishnan, Gokul J.; Yang, Zhen; Li, Zili; Dollevoet, Rolf

DOI
10.1007/978-3-031-66971-2_57

Publication date
2024

Document Version
Final published version

Published in
Advances in Dynamics of Vehicles on Roads and Tracks III

Citation (APA)
Krishnan, G. J., Yang, Z., Li, Z., & Dollevoet, R. (2024). A Concept for Torque Modulation-Based Train-Borne Measurement of Coefficient of Friction. In W. Huang, & M. Ahmadian (Eds.), *Advances in Dynamics of Vehicles on Roads and Tracks III: Proceedings of the 28th Symposium of the International Association of Vehicle System Dynamics, IAVSD 2023, August 21–25, 2023, Ottawa, Canada - Volume 1: Rail Vehicles* (pp. 546-554). (Lecture Notes in Mechanical Engineering). Springer. https://doi.org/10.1007/978-3-031-66971-2_57

A Concept for Torque Modulation-Based Train-Borne Measurement of Coefficient of Friction

Gokul J. Krishnan(✉), Zhen Yang, Zili Li, and Rolf Dollevoet

Delft University of Technology, 2628CN Delft, The Netherlands
{g.jayasreekrishnan,Z.Yang-1,Z.Li,R.P.B.J.Dollevoet}@tudelft.nl

Abstract. The Coefficient of Friction (CoF) is an important parameter affecting acceleration and braking behavior of trains, and consequently the inter-train distance and utilization of track. To optimize operation schedules, maximize railway capacity, and realize automatic train operations, reliable measurements of the CoFs experienced by in-service trains are desirable. In this study, a train-borne measurement approach is proposed based on a torque modulation concept. It involves superimposing a small-amplitude sinusoidal signal on the motor torque. Because the wheel-rail friction force acts as variable damping, it causes a phase difference between the angular velocity response of the wheelset and the input modulated torque signal. This phase difference can be used to determine the creep coefficient, i.e., the slope of the creep curve, and then to estimate the CoF in combination with the measured Coefficient of Adhesion (CoA), i.e., the ratio between the wheel-rail friction force and normal load. Simulations of torque modulation with VI-Rail are conducted. Variation of phase difference with the increase of the modulated torque is derived theoretically and compared with numerically obtained results using the VI-Rail multibody dynamics model under different CoF conditions. The good agreement between the results indicates the effectiveness of the proposed measurement concept.

Keywords: Coefficient of Friction · Measurement · Torque Modulation

1 Introduction

Characterization of wheel – rail friction is of importance to the railway industry, since the trains rely on the friction force, or creep force, between the wheel and rail for traction and braking. The value of the maximum creep force is bounded by the product of the wheel-rail normal load and Coefficient of Friction (CoF). Therefore, when the normal force between wheel and rail is known, the CoF affects the train acceleration behavior and braking distances, and consequently determines the inter-train distance and utilization of track. Hence, a proper control of CoF value is desirable for the rail infrastructure managers and operators. However, due to the open nature of the railway infrastructure, the values of CoF in real-life tracks may vary greatly and depend on a variety of factors at the wheel-rail interface such as surface roughness, contact pressure,

W. Huang and M. Ahmadian (Eds.): IAVSD 2023, LNME, pp. 546–554, 2025.
https://doi.org/10.1007/978-3-031-66971-2_57

rolling velocity, temperature, humidity, characteristics of the interfacial (third body) layers. To guarantee the safety and punctuality of railway operation, the operators generally choose a conservative value of CoF for the calculations of braking distances and scheduling of timetables. For example, the Dutch railway uses a CoF value of 0.15 for timetable schedule calculations [1], even though some experiments have shown that the CoF can be as high as 0.25 for wet contact conditions (water) [2]. This, however, causes an underestimate of railway capacity. To optimize operation schedules, maximize the track capacity, and realize the automatic train operations in the coming 10 to 20 years, a better understanding and reliable measurement of the CoFs experienced by in-service trains are essential**.**

Measurements of CoF have been conducted in labs under controlled conditions using a variety of scaled set-ups (twin-disc [3], pin-on-disc [4], etc.) and full-scale roller rigs [5]. Different wheel-rail contact conditions, including the effects of contaminations, can be studied in such setups [3–5]. Field measurements of CoF are mostly done with hand-operated tribometers [2]. By contrast, train-borne measurements [6] are barely conducted [7], which may, however, provide significantly different results in comparison to the ones measured using hand-operated tribometers [7]. A reliable train-borne measurement is thus desired to obtain the actual CoFs that affect railway operation.

Train-borne measurements of CoF can be done in direct or indirect ways. The direct methods require the measurement of wheel-rail contact force in three directions: normal load, longitudinal and lateral friction force. The Coefficient of Adhesion (CoA), which is the ratio of the tangential force (i.e., the vector sum of the longitudinal and lateral friction force) and the normal load, can then be calculated and is bounded by the CoF. One way to measure the CoF directly is to achieve friction saturation, by detecting wheel slip [7], and then take the measured CoA as the CoF. However, wheel slip introduces large sliding force and creepage, which are detrimental to the train operation and track health condition. To avoid wheel slip, another direct approach based on the creepage measurement was proposed: when the measured creepage value is over a certain threshold value close to friction saturation, the CoA is assumed as CoF [8]. However, this approach relies on the high-precision train-borne measurement of creepage, which is challenging, especially when the creepage value is low [9].

Indirect methods, mainly developed for wheel slip protection systems, combine vehicle and wheel-rail contact models and measured vehicle responses to estimate the CoF based on the parameter estimation algorithms such as Kalman filters [10]. Indirect methods have the advantage in terms of cost and sensor integration into existing vehicle designs. Their main drawback is that the estimation accuracy is highly dependent on the vehicle and wheel-rail contact models used to tune them. Furthermore, such systems are usually optimized for specific CoF values. Hence, ensuring accurate estimation over a wide range of CoF values is difficult. The indirect methods have been validated in the lab setups [11] and numerical simulations [12], but, to the best knowledge of the authors, has not been implemented in the field measurements, because the complexity of the open railway system brings great uncertainty to the parameters involved in the vehicle and wheel-rail contact models [12], and challenges the reliability of indirect methods.

2 Concept of the Torque Modulation Method

In this paper, a new direct train-borne measurement approach is proposed. Instead of relying on the challenging creepage measurement, the proposed method estimates the CoF based on a torque modulation concept [13]. This method was originally developed as a Wheel Slip Protection (WSP) algorithm. It involves superimposing a small-amplitude sinusoidal signal on the motor torque signal. The wheel-rail creep force acts as a variable damper, and causes a phase difference between the measured angular velocity response of the wheelset and the input modulated torque signal. This phase difference determines the slope of the creep curve, i.e., creep coefficient, at the operating point of the wheelset. An example is shown in Fig. 1, which considers a half wheelset rolling on a straight track at constant velocity of v. The rolling radius is R and the angular speed of the wheelset is Ω. The longitudinal suspension force is shown as $f_{x-suspension}$ in Fig. 1 (a), which is assumed to keep the wheel rolling at a constant velocity. The normal load on the contact is denoted by N.

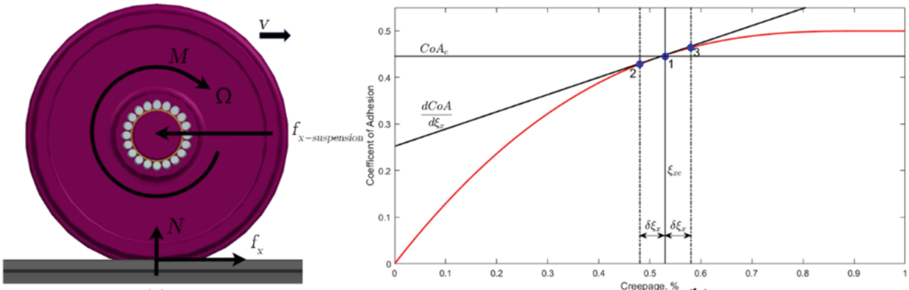

Fig. 1. An example of (a) a half-wheelset rolling on a straight track (b) creep coefficient at the operating point

A modulated torque is then applied given by

$$M = M_c + M_0 \sin(\omega_m t) \tag{1}$$

where M_c is the constant torque (DC level) and M_0 is the magnitude of the modulating torque. The corresponding operating point at the DC level is shown on the creep curve (Fig. 1 (b)) and labelled “1”. Due to the modulation, the creepage and CoA vary and accordingly the operating point oscillates along the creep curve between the points “2” and “3”. When the forced torsional oscillation of the wheelset takes place with a frequency of ω_m, the angular velocity of the wheelset with the modulation torque is given by

$$\Omega = \Omega_c + \Omega_0 \sin(\omega_m t + \phi) \tag{2}$$

where Ω_c is the DC level, and Ω_0 is the amplitude of the angular velocity oscillation and ϕ is the phase difference with the modulation torque. Assuming only the longitudinal creepage (ξ_x) exists, the rotational equation of motion of the half-wheelset can be solved, which yields the following equation for the phase difference ϕ.

$$\tan\phi = \frac{I_w \omega_m v}{NR^2 \frac{d(CoA)}{d\xi_x}} \tag{3}$$

where I_w is the moment of inertia of the half wheelset, and $\frac{d(CoA)}{d\xi_x}$ is the slope of the creep curve at the operating point, i.e., the creep coefficient as shown in Fig. 1 (b). Thus, the measurable phase difference between the modulated torque signal and the response angular velocity of the wheelset is inversely proportional to the creep coefficient. When approaching friction saturation, the creep coefficient tends to zero, and the corresponding phase difference moves towards 90° according to Eq. (3). By setting certain threshold for the measured phase difference, we can ensure that the operating point is close to saturation, and not exceed it. Then, the measured CoA can be taken as the CoF.

3 Simulation Methodology

The method proposed in Sect. 2 is derived based on a single half wheelset model (Fig. 1 (a)). Previous studies have simulated stand-alone single wheelset dynamics with torque modulation for WSP systems [14]. However, the effects of vehicle (including bogie and car body) dynamics have not been considered. In order to implement the method in real-world settings of railway vehicles, the modulation-based measurement applied to a single wagon model travelling on a straight track is simulated with the multibody dynamics software VI-Rail, as shown in Fig. 2.

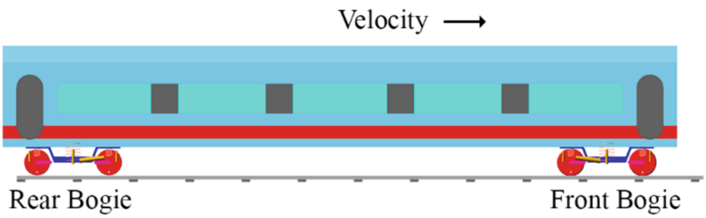

Fig. 2. The ERRI wagon model used for simulation.

The template model "ERRI wagon" is used in the simulation. In order to control the wheelset torque, a point torque actuator is added to the rear wheelset of the rear bogie. To maintain the velocity of the wagon as constant as possible under the torque modulation condition, an equal but opposite point torque actuator is added to the front wheelset of the same bogie, and a cruise control setting is used which employs a Proportional-Derivative (PD) controller that takes a certain set point velocity as input, and tries to maintain this velocity by applying appropriate forces to the car body to cancel out any accelerations.

In order to assess the robustness of the method, simulations are performed with different CoF values. The simulation results are then analyzed and compared with the theoretical results/trends predicted by Eq. (3).

4 Results

4.1 Progression of Phase Difference with Increase of the Modulated Torque

Figure 3 shows an example of the modulated torque signal applied to the VI-Rail model and the resulting angular speed of the wheelset. The applied torque is gradually increased from zero to a steady state DC value M_c, which is 20946 Nm in this case. Then, a modulation signal is applied, with the amplitudes M_0 and frequency ω_m of the modulated torque being 345 Nm and 5 Hz, respectively. In order to extract the phase difference between the modulated torque and angular speed signals, the signals are high-pass filtered to remove the DC component. Then, a sine fitting algorithm [15] is used to estimate the phase difference of the filtered signals.

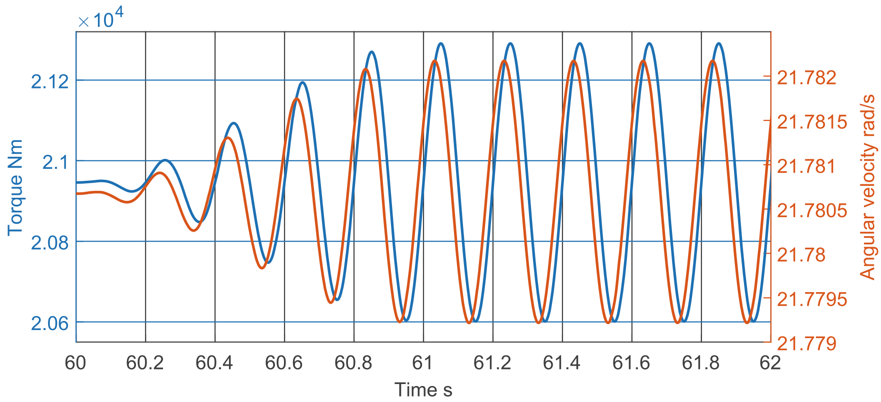

Fig. 3. Applied torque modulation signal (blue) and the resulting wheel angular velocity (orange)

The simulations are conducted in VI-Rail with an increase of the DC value of the modulated torque from 1% of the saturation torque value with a step of 10% until friction saturation is reached. The step size is made finer towards the saturation torque, with step size reducing to 5% after 50% of saturation torque, to 3% after 70% of saturation torque, and to 1% after 90% saturation torque.

The computed phase difference values for a CoF of 0.4 is shown in Fig. 4 as a function of the applied torque, represented by a percentage of the saturation torque. The normal load N is set as 100 kN. The simulated modulation frequency ω_m is 5 Hz, and the train speed v is10 m/s.

According to Eq. (3), when the operating point approaches the saturation, the phase difference tends to 90°. The variation is highly non-linear with a rapid increase after 94% of saturation torque as plotted in Fig. 5, which is in line with the simulation results presented in Fig. 4. The moment of inertia I_w is set as 116 kg m^2, and the rolling radius R is 0.46 m.

However, a major difference between the theoretical result and simulation result is noticeable: at torque values before 94% saturation torque, Eq. (3) predicts a phase difference close to zero, as the product of creep coefficient $\frac{d(CoA)}{d\xi_x}$ and the normal load N

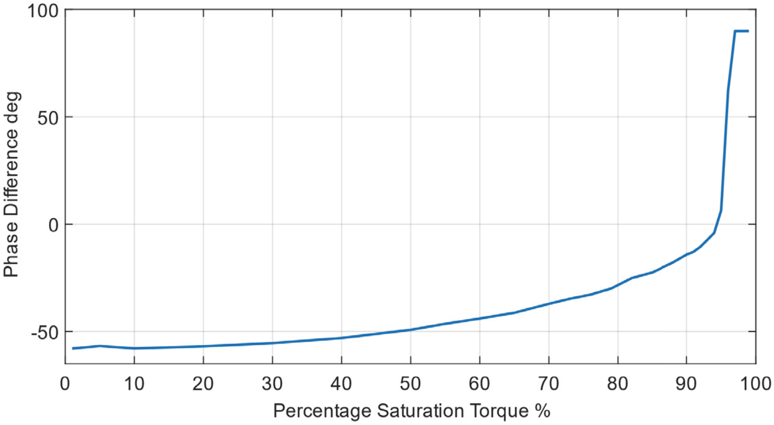

Fig. 4. Phase difference progression for the simulation case CoF = 0.4

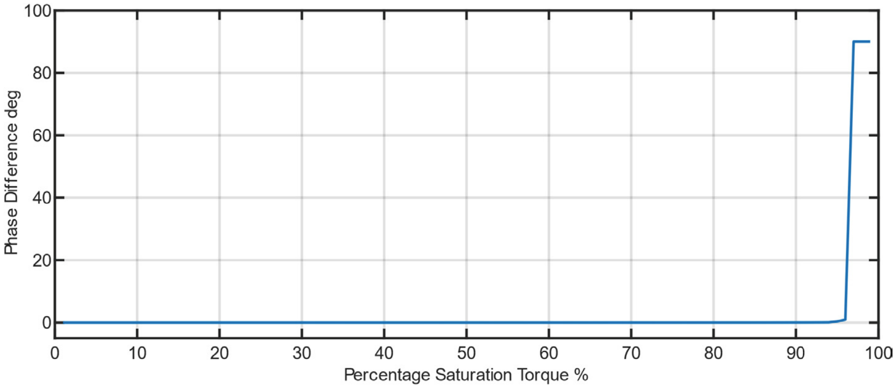

Fig. 5. Theoretically predicted progression of phase difference as per Eq. (3)

are much higher than the numerator $I_w \omega_m v$, due to the large slope of the creep curve at low creepage, whereas in the simulation results, a negative phase difference is observed at these torque values. This difference is believed to be due to the velocity profile of the wagon.

The theoretical model defined by Eq. (3) assumes that the train speed is constant, and thus the creepage and the angular velocity of the wheelset are in phase. This is, however, not the case for the VI-Rail simulation. Due to the cruise control simulated in VI-Rail, the train travel velocity exhibits oscillations. The amplitude of the oscillation is so small that the speed magnitude can be considered constant in the cruise control simulation. However, the oscillation introduces an additional phase component to the longitudinal creepage ξ_x, resulting in that the longitudinal creepage and the wheelset angular velocity Ω simulated with VI-Rail are out of phase, as shown in Fig. 6.

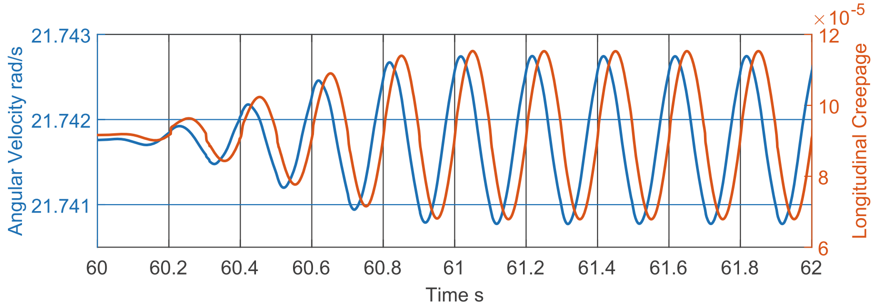

Fig. 6. The longitudinal Creepage (orange) and wheelset angular velocity (blue) signal

If we consider this phase difference between ξ_x and Ω to be ϕ_v, then Eq. (3) can be modified to

$$\tan\varphi = \frac{I_w \omega_m v}{NR^2 \frac{d(CoA)}{d\xi_x} \cos(\phi_v)} - \tan(\phi_v) \tag{4}$$

Now, we can see that at low torque values, the first term vanishes, and the phase difference between the torque and wheelset angular velocity is equal to the additional phase difference introduced. Figure 7 plots Eq. (4) and the simulated phase difference (as shown in Fig. 4). The good agreement between the theoretical and simulation results validates the effectiveness of the modulation-based measurement method.

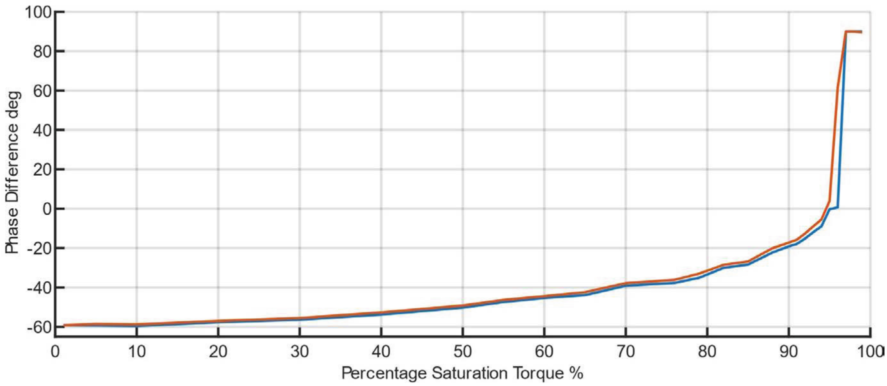

Fig. 7. Theoretical phase difference progression as per Eq. (4) (blue) and simulated phase difference progression (orange)

4.2 Variation with CoFs

Simulations are then repeated for different CoF values from 0.1 to 0.5 with a step of 0.1. The CoF is not involved in Eq. (4), and thus, should not affect the phase difference progression. As shown in Fig. 8, the results simulated with different CoFs exhibit the same trend, with some differences in the low torque region. The differences are attributed to the difference in the velocity controller action, which changes the second term in Eq. (4). Figure 8 also shows that almost all curves of phase difference progression cross zero phase difference at around 94–95% saturation torque. This can be a potential threshold value to estimate CoF. Namely if we increase the DC component of the applied modulation torque in steps, when the measured phase difference has become positive, the measured CoA can be taken as the CoF, with an expected error of 5%.

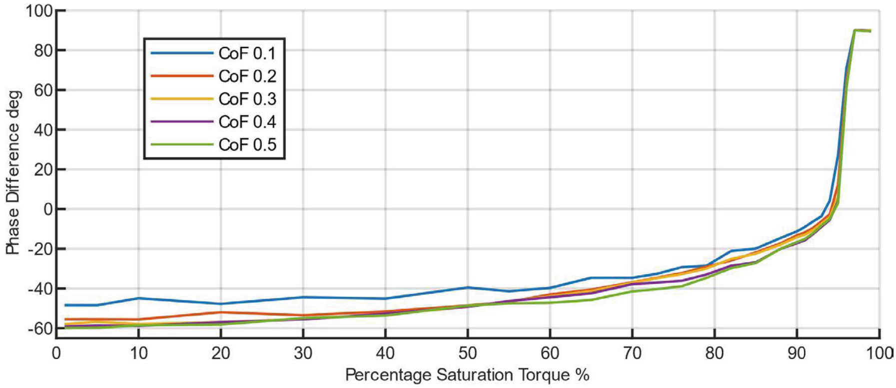

Fig. 8. Phase difference progression for different CoFs

5 Conclusions and Outlook

The torque-modulation based method was proposed as an alternative to the challenging creepage measurement-based methods for the direct measurement of CoF. Application of torque modulation on a single half wheelset was first analyzed to demonstrate the variation of the phase difference between the modulated torque and the wheelset angular velocity, and the creep coefficient at the operating point. The effectiveness of the concept was then numerically validated with a VI-Rail wagon model. The simulation results indicate that the CoA can be taken as the CoF, with an expected error of 5%, when the phase difference transitions from negative to positive with an increase of the modulated torque value.

To put the method to the practical application, the following challenges needs to be responded to: constant train velocity, traction motor control, potential discomfort to the passengers, and a reliable measurement of the wheel-rail contact forces. In addition, the present study focused on the development a CoF measurement algorithm on straight tracks and thus neglected lateral creepage at the wheel-rail contact, which can be significant in curves. Further research will address the effect of curving behavior and parameter (such as wheel torque, angular velocity and phase difference) resolutions on the measurement algorithm, and for practical implementation, a train-borne instantaneous contact force measurement system will be developed. As an alternative to sinusoidal torques, other interrogation signals will be explored, which can potentially be used to estimate CoF at lower magnitudes of applied torque. Experimental validation of the principle applied to a single half wheelset will also be conducted using the V-Track test rig at TU Delft [16].

References

1. Popovici RI (2010) Friction in wheel-rail contacts. Ph.D. thesis, University of Twente
2. Areiza, Y.A., Garcés, S.I., Santa, J.F., et al.: Field measurement of coefficient of friction in rails using a hand-pushed tribometer. Tribol. Int. **82**, 274–279 (2015)
3. Fletcher, D.I., Lewis, S.: Creep curve measurement to support wear and adhesion modelling, using a continuously variable creep twin disc machine. Wear **298–299**, 57–65 (2013)
4. Olofsson, U., Sundvall, K.: Influence of leaf, humidity and applied lubrication on friction in the wheel-rail contact: Pin-on-disc experiments. Proceedings of the Institution of Mechanical Engineers, Part F: Journal of Rail and Rapid Transit **218**, 235–242 (2004)
5. Zhang, W., Chen, J., Wu, X., Jin, X.: Wheel/rail adhesion and analysis by using full scale roller rig. Wear **253**, 82–88 (2002)
6. Watkins, D.J.: Exploring adhesion with British Rail's tribometer train. Railway Eng. J. **4**(4), 6–13 (1975)
7. Lundberg, J., Rantatalo, M., Wanhainen, C., Casselgren, J.: Measurements of friction coefficients between rails lubricated with a friction modifier and the wheels of an IORE locomotive during real working conditions. Wear **324–325**, 109–117 (2015)
8. Petrov, V., Berg, M., Persson, I.: Estimation of wheel–rail friction for vehicle certification. Veh. Syst. Dyn. **52**, 1099–1114 (2014)
9. Giner, J., Baeza, L., Vila, P., Alonso, A.: Study of the Falling Friction Effect on Rolling Contact Parameters. Tribol. Lett. **65**, 29 (2017)
10. Shrestha, S., Wu, Q., Spiryagin, M.: Review of adhesion estimation approaches for rail vehicles. International Journal of Rail Transportation **7**, 79–102 (2019)
11. Schwarz, C., Keck, A.: Simultaneous Estimation of Wheel-Rail Adhesion and Brake Friction Behaviour. IFAC-PapersOnLine **53**, 8470–8475 (2020)
12. Hussain, I., Mei, T.X., Ritchings, R.T.: Estimation of wheel–rail contact conditions and adhesion using the multiple model approach. Veh. Syst. Dyn. **51**, 32–53 (2013)
13. Pichlík, P.: Summary of the Modern Wheel Slip Controller Principles. TEE **8**, 26–31 (2020)
14. Pichlík, P.: Overview of Slip Control Methods Used in Locomotives. Transactions on Electrical Engineering **3**, 38–43 (2014)
15. Ramos P. M., Da Silva F., Cruz Serra V: Improving sine-fitting algorithms for amplitude and phase measurements phase measurements, Proc. of XVII IMEKO World Congress, Dubrovnik, June 2003, pp. 614- 619
16. Zhang, P., Moraal, J., Li, Z.: Design, calibration and validation of a wheel-rail contact force measurement system in V-Track. Measurement **175**, 109105 (2021)